



UNIVERSITY OF LEEDS

This is a repository copy of *Effect of mechanical vibration on the size and microstructure of titania granules produced by auto-granulation*.

White Rose Research Online URL for this paper:
<http://eprints.whiterose.ac.uk/89285/>

Version: Accepted Version

Article:

Ku, N, Hare, CL, Ghadiri, M et al. (2 more authors) (2015) Effect of mechanical vibration on the size and microstructure of titania granules produced by auto-granulation. *Powder Technology*, 286. 223 - 229. ISSN 0032-5910

<https://doi.org/10.1016/j.powtec.2015.05.041>

© 2015, Elsevier. Licensed under the Creative Commons Attribution-NonCommercial-NoDerivatives 4.0 International
<http://creativecommons.org/licenses/by-nc-nd/4.0/>

Reuse

Unless indicated otherwise, fulltext items are protected by copyright with all rights reserved. The copyright exception in section 29 of the Copyright, Designs and Patents Act 1988 allows the making of a single copy solely for the purpose of non-commercial research or private study within the limits of fair dealing. The publisher or other rights-holder may allow further reproduction and re-use of this version - refer to the White Rose Research Online record for this item. Where records identify the publisher as the copyright holder, users can verify any specific terms of use on the publisher's website.

Takedown

If you consider content in White Rose Research Online to be in breach of UK law, please notify us by emailing eprints@whiterose.ac.uk including the URL of the record and the reason for the withdrawal request.



eprints@whiterose.ac.uk
<https://eprints.whiterose.ac.uk/>

Effect of mechanical vibration on the size and microstructure of titania granules produced by auto-granulation

Nicholas Ku, Colin Hare, Mojtaba Ghadiri, Martin Murtagh, Richard A. Haber

Abstract

Auto-granulation is the growth of particle clusters within a dry, fine powder bed due to the bulk powder cohesion. This clustering occurs without the addition of any binder to the system due to simple agitation of a powder, such as during storage or handling. For this reason, it is important in powder processing to be able to characterize this behavior. In this study, a sub-micron titania powder is mechanically vibrated under controlled conditions to induce clustering and promote auto-granulation. The amplitude and frequency of the vibration is varied to view the effect on the equilibrium granule size. A statistical model of the effect is also developed to determine that the granule size increases linearly with vibrational energy. Furthermore, imaging of cross-sections of the granules is conducted to provide insight into the internal microstructure and measure the packing fraction of the constituent particles. It is found that under all vibrational conditions investigated the particles exhibit a core-rim microstructure.

1. Introduction

When dealing with fine powders, as the particle size is reduced, the attractive interaction between particles increases in significance, dominating over the effect of gravitational forces. This leads to an increase in powder cohesion with finer sizes, and promotes a behavior where the

small particles cluster into larger agglomerates [1]. Increasing the propensity of a powder to agglomerate can cause difficulties in powder flow and lead to problems during storage and handling [2]. This behavior of size enlargement is common in many powder processes [3, 4]. For this reason, there is an industrial interest to be able to understand how size enlargement of powders occurs under given conditions.

A process conducted specifically to induce size enlargement in a powder is known as granulation. The most common methods include the addition of a wetting agent or binder solution to the powder to promote the clustering of particles [5]. Auto-granulation is a granulation process that occurs within a fine powder without any additives. The powder clusters simply become loosely bound due to the highly cohesive nature of the inter-particle contacts. Ku et al. [6] found that auto-granulation can be induced in a powder by agitating the powder bed using mechanical vibration. For a given vibrational amplitude and frequency, the powder clusters to a maximum equilibrium size with an inherent strength. This equilibrium size is dependent on the mechanical vibration intensity. While Ku et al. [6] observed a general trend of equilibrium granule size with vibrational intensity, the significant parameter of the mechanical vibration was not statistically verified, nor the actual dependence calculated.

The process of how the powder forms clusters during auto-granulation is not completely understood. In traditional wet granulation, the theory at the micro-level involves two competing factors: the energy dissipation of the binder layer and the rebounding kinetic energy of the collision between two colliding particulate units. The mechanism of growth occurs due to the coalescence of like-sized particulate units, such as particles-to-particles, agglomerates-to-agglomerates, or granules-to-granules [7]. This would result in a hierarchical microstructure, where the internal structure exhibits the multi-scale growth process. Such granules would be

visibly comprised of clusters, with those clusters formed from smaller clusters. This results in a pattern that continually reduces in scale until small clusters comprised of individual particles are observed.

Without the presence of a viscous binder layer, there is limited ability to dissipate the collision energy between two like-sized particulate units, and the collision would most likely result in rebound [3]. Therefore, it is unlikely the theory presented by Ennis et al. [7] can be applied to explain the auto-granulation process, where the particles are dry and there is no binder present. The mechanism of growth during auto-granulation was proposed by Ku et al. [6] to be a snow-balling process, where fine particles are consumed by larger granules by sticking onto their surface. As more fine particles stick to the surface of the granule, the granule grows [6]. This snow-balling process would produce a homogeneous microstructure, as the granules would be comprised of a singular sized building block: the fine particles of the powder.

Similarly to auto-granulation, pressure swing granulation is also a binderless granulation process that produces granules with an inherent strength. In pressure swing granulation, the powder is placed in a fluidized bed column and the air flow within the column is cyclically changed between a compacting, downward flow and fluidizing, upward flow through the bed [8]. The granules produced by this method exhibit a microstructure with a core-rim structure, where the surface of the granules has a denser particle packing than the core [9]. Horio [9] theorized that the motion of the granules around the chamber during the fluidization step leads to surface deformation of the granules, creating the denser outer shell. This denser outer shell also explains the increased strength of the granules over the bulk powder bed, as the increased packing fraction at the surface creates an increased mechanical strength [9].

Golchert et al. [10] investigated the effect of granule microstructure on the compressive strength of the granule. This study suggested a heavy dependence on both the type and extent of breakage experienced by the granule. The propagation of cracks was shown to be dependent on the network of contacts between the particles within a granule [10]. Therefore, the ability to characterize the internal microstructure of a granule is of extreme importance to understand the granule strength.

Models to predict granule size in vibro-fluidized beds have been shown using both a force balance [11] and an energy balance [12] approach. In a vibro-fluidized bed, the bulk powder is subjected to a fluidized air flow along with the mechanical vibration [11]. This creates a different environment to a simply mechanically vibrated powder bed, with the absence of fluidizing air flow. While studies have been made into the behavior of powder beds under mechanical vibration [13, 14], none have observed or characterized auto-granulation behaviour of the powder.

The main aim of this study is to determine the effect the mechanical vibration has on the auto-granulation behavior. This is achieved by statistically determining the significant parameter of the mechanical vibration on the equilibrium granule size. Furthermore, the internal microstructure of the formed granules is imaged to provide insight into the mechanism of granule growth.

2. Experimental setup and methodology

Material system

The powder sample used for this study was AT1 titanium dioxide powder, supplied by Cristal Global. This powder is made of smooth, spherical primary particles with a size of

roughly 100 nm, as shown in Figure 1. The appearance of the powder is white and cohesive, with loose clusters easily forming during powder handling and storage. For each test, the mass of the powder used was kept constant at 15g. To test the powder at a reproducible state, a preconditioning step was used where the powder was sieved through a 1.4 mm (14 mesh) sieve to break up any large clusters before testing.

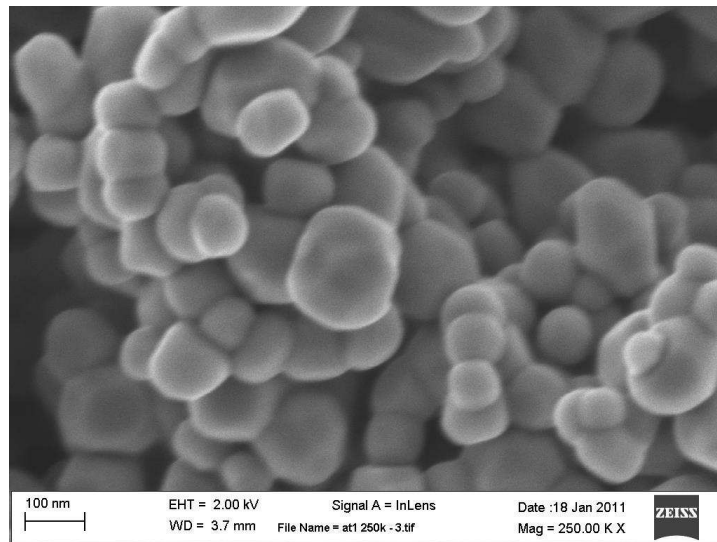


Figure 1. SEM image showing particles of Cristal Global AT1 titania powder.

Mechanical vibration

An electrodynamic shaker (The Modal Shop Inc. K2007E01) was used to apply the mechanical vibration to the powder bed. A schematic diagram of the experimental setup is shown in Figure 2. A signal generator creates a digital, sinusoidal wave, which is converted to a mechanical vibration by the electrodynamic shaker. The powder is placed in an acrylic box with length and width of 60 mm, which is vibrated by the electrodynamic shaker in a vertical motion.

The motion is monitored using a high speed camera to ensure the correct frequency and amplitude is applied to the powder bed and to observe the auto-granulation process.

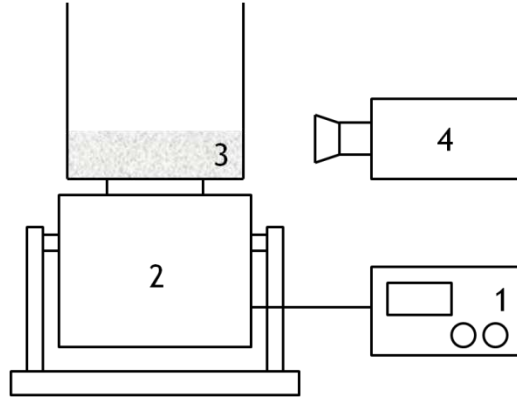


Figure 2. Experimental setup showing the (1) signal generator, (2) electrodynamic shaker, (3) powder bed in acrylic container, and (4) high speed camera.

For this study, a range of vibration frequencies and amplitudes were used, as shown in Table 1. The amplitude and frequency of each test condition was converted to a vibration energy, E , using simple harmonic motion (Eq. 1).

$$E = \frac{1}{2}kA^2 = 2m(\pi fA)^2 \quad (1)$$

where k is the wave number, A is the amplitude, m is the mass of the sample, f is the frequency and acceleration, a , and power, P , are given by equations 2 and 3, respectively.

$$a = A(2\pi f)^2 \quad (2)$$

$$P = Ef = 2mf^3(\pi A)^2 \quad (3)$$

For test conditions 1-4, the amplitude of the vibration was kept constant at 1.00 mm and the frequency was varied from 35 to 50 Hz. For test condition 5, the frequency was held at 50

Hz but the amplitude was changed to 0.80 mm to create a vibration with an energy equal to test condition 2. Likewise, in test condition 6 the frequency was held constant but the amplitude was changed to 0.64 mm to create a vibrational acceleration equal to test condition 2. A vibration time of 20 minutes was used for all test conditions, since the granules were found to grow to their equilibrium size by this point [6].

Table 1. Test conditions for mechanical vibration of the powder.

Test condition	Frequency(Hz)	Amplitude (mm)	Energy (J)	Acceleration (m/s ²)	Power (W)
1	35	1.00	0.0056	48.36	0.20
2	40	1.00	0.0073	63.17	0.29
3	45	1.00	0.0092	79.94	0.41
4	50	1.00	0.0114	98.70	0.57
5	50	0.80	0.0073	78.96	0.36
6	50	0.64	0.0046	63.17	0.23

Granule sizing

After mechanical vibration of the powder, the granules formed were gently poured from the acrylic box to be collected. The size of the granules was then measured by gently scattering the granules over a flat surface and taking a high-resolution, overhead image of the entire population. The images had a pixel size of 0.058 mm. The images of the granules were analysed using ImageJ, with the pixel area of each granule being measured and converted to a diameter of a sphere of equivalent projected area. Using this optical method, the size of the granule population was measured as a number distribution. A model of the granule size as a

function of the mechanical vibration was constructed, investigating vibrational energy, acceleration, and power separately. The statistical significance of data was analyzed using Minitab 17.1.0.0 by Minitab Inc.

Heat treatment for infiltration

Imaging of fragile structures provides a unique problem in finding a way to preserve the internal microstructure during sample preparation for microscopy. Embedding the sample in an epoxy resin is a solution to the sample preparation problem [15]. The epoxy resin has a low viscosity before curing, allowing for complete infiltration into the pores within the granule. To prevent the granule from dispersing when immersed in the liquid resin, the granules were heat treated to create necking between particles to increase mechanical strength [16].

The goal of the heat treatment was to increase the mechanical strength of the granules to survive the epoxy infiltration procedure, but not to alter the microstructure of the granules in the process. The granules were heat treated in an alumina boat with a box furnace. The temperature was increased at 10°C/minute to various target temperatures: 700°C, 800°C, and 900°C. The sample was held at the target temperature for a dwell time of 60 minutes. The furnace was then cooled back to room temperature at a rate of 25°C/minute.

The effects of the various heat treatments were compared using two methods; granule immersion in water and SEM imaging of granule fragments. Granules were immersed in water to observe if they had sufficient strength to resist dispersion in a dispersing fluid. For SEM imaging, granules were broken into fragments after heat treatment and fixed to an SEM sample

stud using colloidal silver paste. The fragments were imaged to view if there were any observable changes to the primary particles, such as grain growth, due to the heat treatment.

Sample preparation and imaging

The epoxy used for sample preparation was the Ted Pella, Inc. Spurr Low Viscosity Kit, which mixes in a liquid state and hardens with exposure to heat. The low viscosity epoxy resin allows for infiltration into the interparticle pores within the granule without dispersion or breakage. The epoxy was mixed using the following recipe: 4.10 g of ERL 4221, 1.90 g of diglycidylether of polypropyleneglycol (DER 736), 5.90 g of nonenyl succinic anhydride (NSA), and 0.10 g of dimethylaminoethanol (DMAE). The mixed epoxy resin was then placed in a Buehler Cast N' Vac 1000 castable vacuum system with the heat treated granule under a vacuum of 660 mmHg. After allowing 60 minutes to ensure any bubbles formed within the epoxy due to mixing had dissipated, the epoxy was poured slowly on top of the granule sample under vacuum. The sample was then kept under vacuum a further 60 minutes after combining the epoxy and granule. Upon removing the sample from vacuum, the sample was placed in an oven at 60°C for 12 hours to allow the epoxy to cure.

After epoxy infiltration, the samples were polished to expose the hemispherical plane of the granule. Polishing was conducted using a 0.05 μm diamond suspension to polish through the epoxy and particles to create a flat, 2-dimensional cross-section of the granule. The sample was then coated with a 5nm layer of gold to minimize charging of the sample in the SEM. Imaging in the SEM was conducted using the in-lens detector, which allows for a compositional contrast

to distinguish between particles and epoxy. A gun voltage of 5kV was used to minimize charging but maintain compositional contrast.

3. Results and discussion

Granule size

For each test condition, the entire population of granules produced by auto-granulation was optically imaged and sized. The sizes of the granules produced for all test conditions are shown as a function of energy, acceleration and power in Figure 5, respectively. The size was measured as the diameter of a sphere with equivalent projected area and represented as the d_{10} , d_{50} , and d_{90} of the number distribution of the population. Three repeats of each test condition were made, with each data point denoting the average and the bars showing the range of the three measurements.

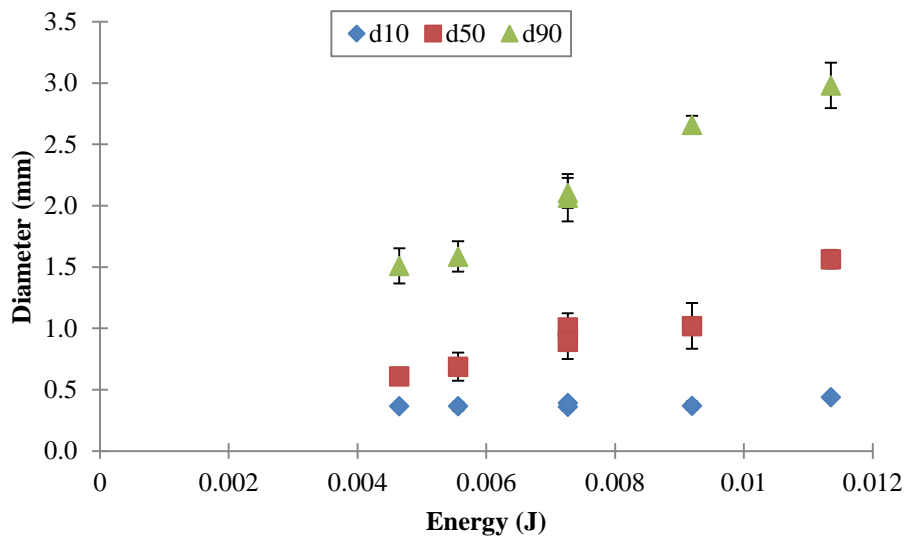


Figure 3. Diameter of produced granules as a function of the vibrational energy.

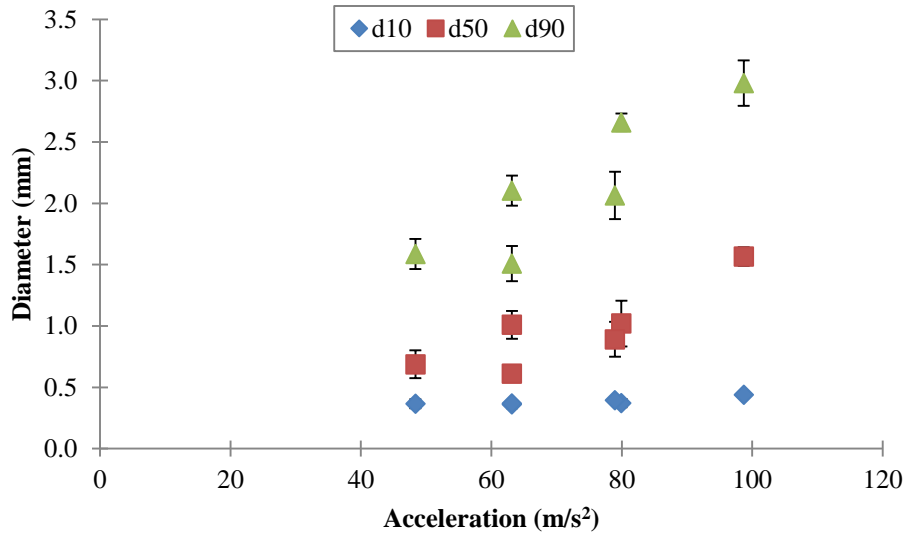


Figure 4. Diameter of produced granules as a function of the vibrational acceleration.

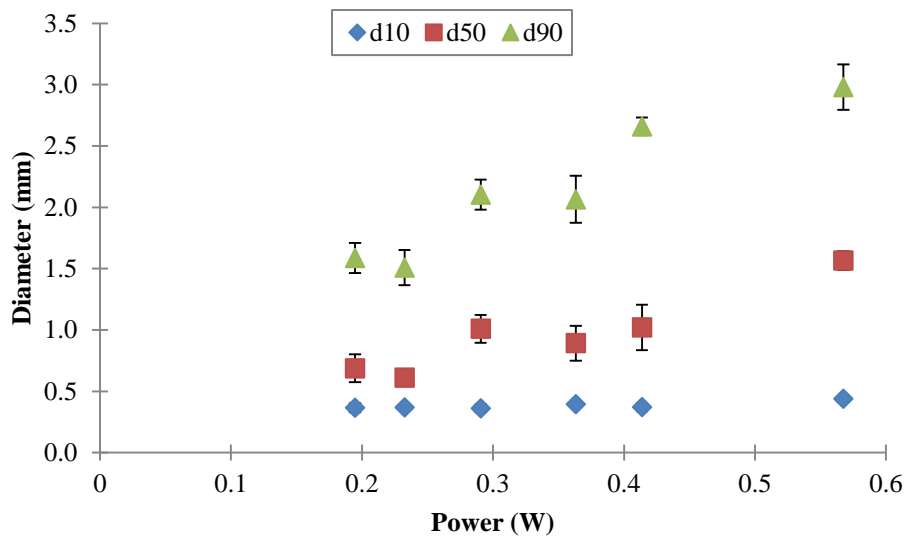


Figure 5. Diameter of produced granules as a function of the vibrational power.

There is a general increasing trend of granule size with increasing vibration intensity, regardless of whether the intensity is considered in terms of energy, acceleration, or power. The largest dependence on vibration intensity is observed in the d_{90} of the size distribution, with the d_{10} and d_{50} showing a less sharply increasing trend. Thus, the d_{90} data was chosen to fit to a linear model.

Table 2. Statistical significance of linear fit of vibrational intensity parameters to granule size.

Parameter	R^2
Energy (J)	0.98
Acceleration (m/s^2)	0.91
Power (W)	0.78

The R^2 value of each linear fit of vibrational intensity parameter to the d_{90} of the granule size is shown in Table 2. As the criteria for statistical significance is an R^2 value that is greater than 0.95 [17], only the linear fit of the energy parameter is statistically significant. The linear fit is shown in Equation 4, where d_{90} is the 90th percentile of the granule diameter distribution and E is the vibrational energy. The regression analysis of the linear model yielded a p-value of 0.044 for the constant term, and a p-value of 0.010 for the energy coefficient. As both p-values are less than 0.050, a rejection of the null hypothesis is made [17] and both terms are presumed to be significant to the linear model.

$$d_{90} = 0.367 + 236.3E \quad (4)$$

Heat treatment

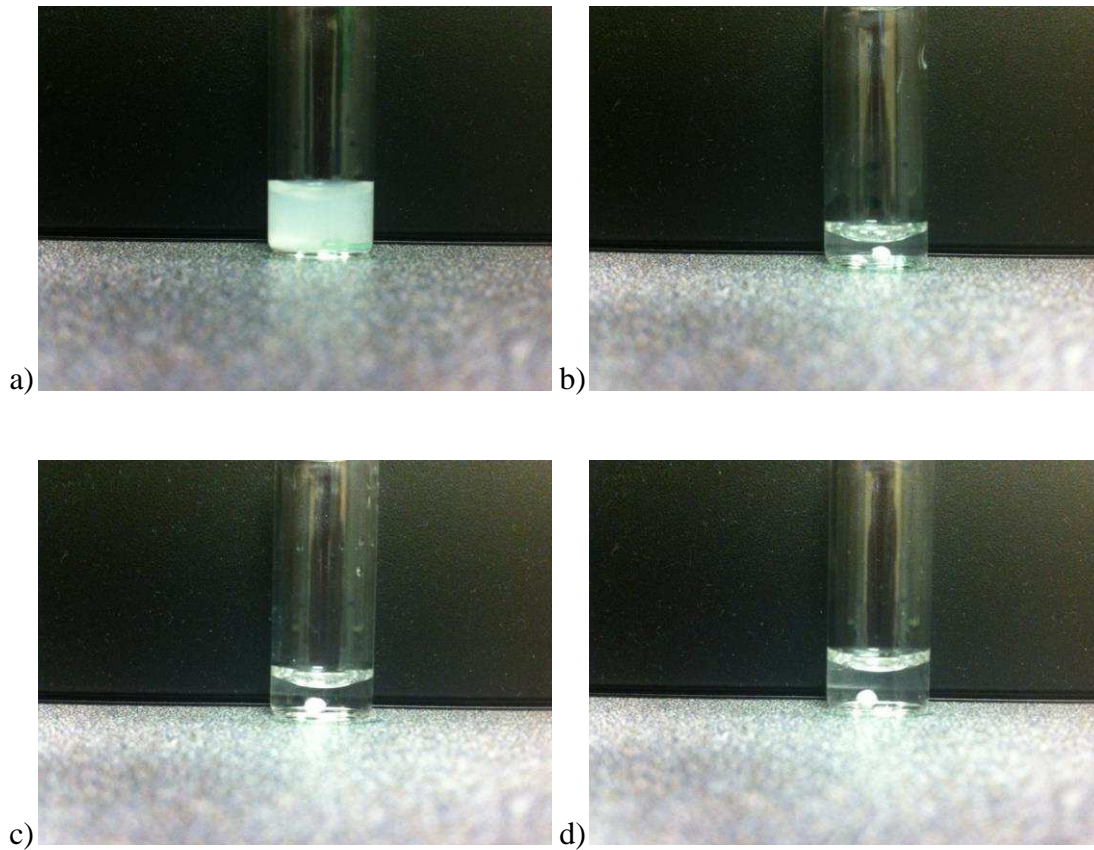


Figure 6. Granules (a) with no heat treatment, (b) heated to 700°C, (c) heated to 800°C, and (d) heated to 900°C immersed in water.

The results of immersing the heat treated granules in water are shown in Figure 6. With no heat treatment, the granule easily dispersed when submerged in water. With a heat treatment to a target temperature of 700°C, the granule fragmented into several pieces upon immersion. The granules heat treated to 800°C and 900°C were unaffected by the water. Therefore, granules heat treated up to 700°C would not survive being immersed in the liquid epoxy resin but those treated to 800°C or higher have the ability to survive the infiltration process.

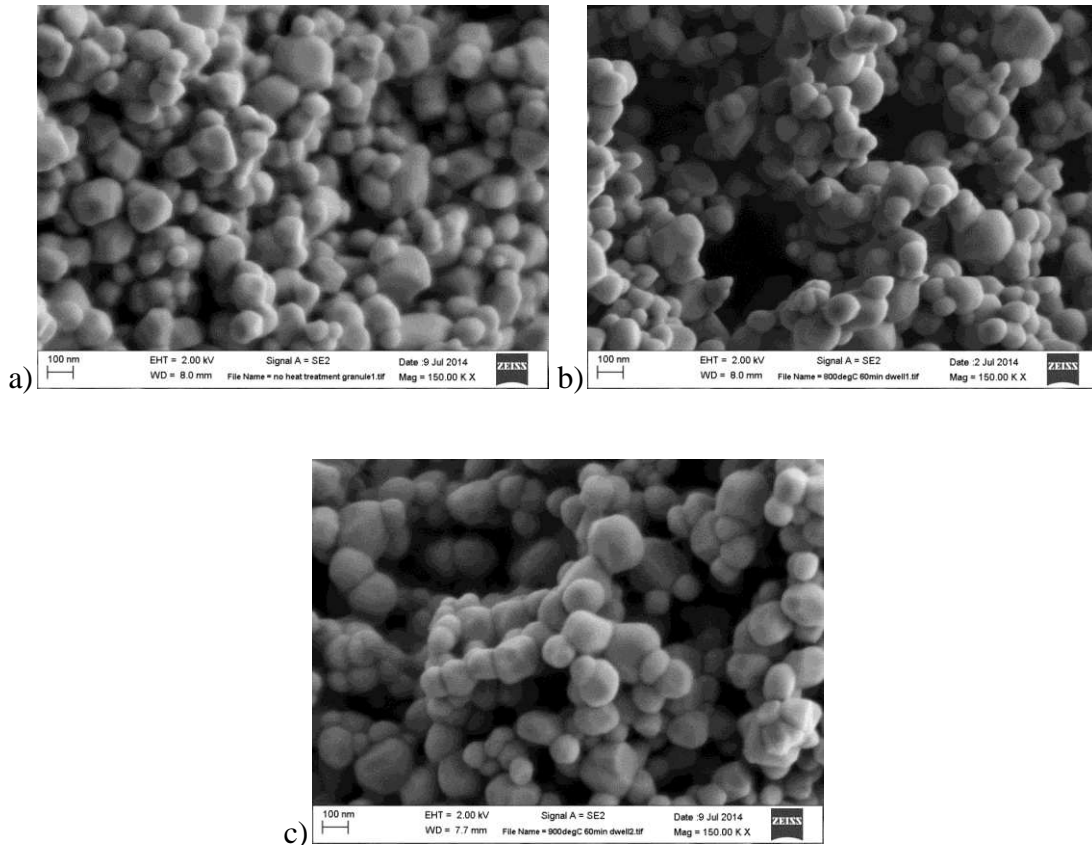


Figure 7. SEM imaging of primary particles of granule fragments after (a) no heat treatment, (b) heated to 800°C, and (c) heated to 900°C.

Granules that underwent heat treatments at 800°C and 900°C were broken into fragments to view if the heat treatment had any visible effect on the size or shape of the constituent particles. Images of the particles within the granules after heat treatment at the two temperatures were compared to the particle within an untreated granule, as shown in Figure 7. No visible sign of particle growth or shape change was evident in the images. Due to this SEM imaging and the results of the immersion of granules in water, it was determined that the heat treatment at 800°C and 900°C had no effect on the microstructure within the granule, other than creating

interparticle necks at particle contacts to increase the granule strength. The subsequent heat treatment of granules for epoxy infiltration in this study used a target temperature of 900°C.

Granule microstructure

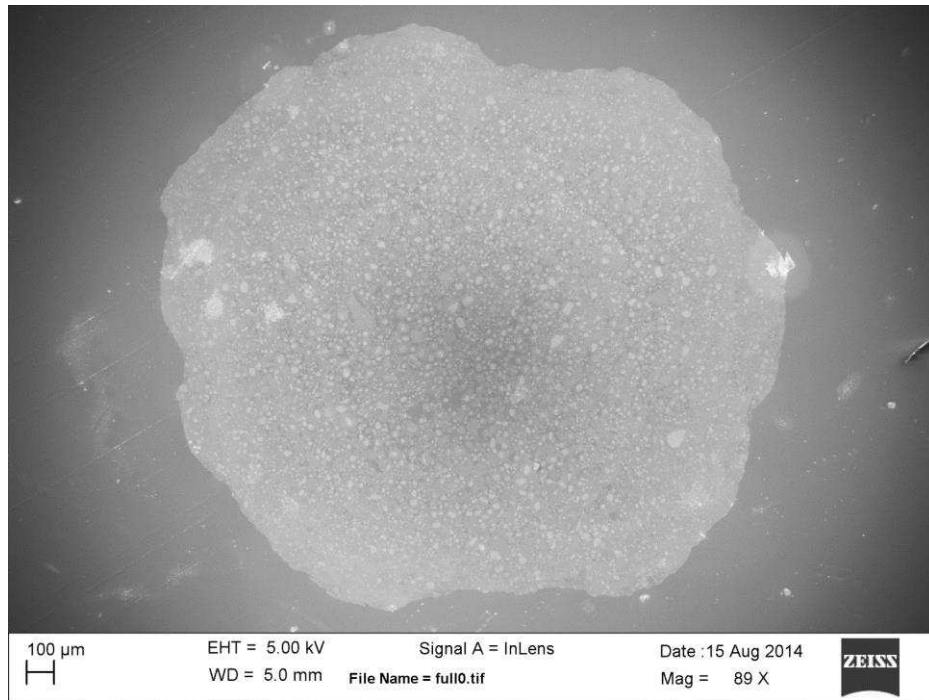


Figure 8. Infiltrated and polished cross-section of granule formed under 40Hz and 1mm amplitude vibration.

An SEM image of the granule cross-section is shown in Figure 8. Due to the compositional contrast provided by the in-lens detector, particles within the granule appear brighter, while the epoxy resin occupying the pores within the granule appears darker. From the image, it is clear that the granule does not have a homogeneous microstructure. The multiple lighter and darker regions seen in the cross-section imply the granule was not produced by a

uniform “snow-balling” of fine particles, but a multi-scale structure of smaller clusters of particles comprising the larger granule. However the higher magnification image of Figure 9 indicates that a mixture of fines and small clusters exists within the granule structure.

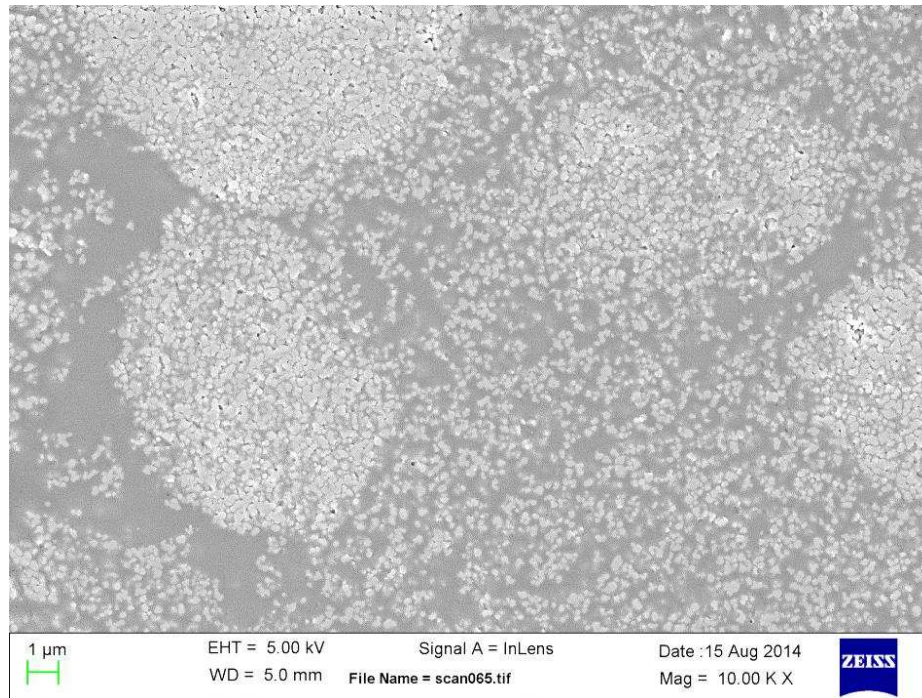


Figure 9. Image of granule cross-section at 10,000× magnification showing individual primary particles of the 40Hz and 1mm amplitude granule sample.

Looking at the higher magnification image of the surface of the cross-section shown in Figure 9, it is apparent that the epoxy resin has completely infiltrated the pores of the particle structure. With polishing, the structure of the granule had been maintained with no significant damage to the granule structure. The area of the image is roughly 27 μm by 27 μm. To view how the microstructure of the granule changes across its width, a series of images was taken over the horizontal diameter of the cross-section using the same magnification. Images were then spliced together to create a mosaic view of the granule microstructure. Figure 10 shows the first

three images of the surface of the granule. The particles were configured with a high packing fraction, creating a dense outer shell on the granule. Conversely, the center three images of the granule (Figure 11) show a much looser pack configuration.

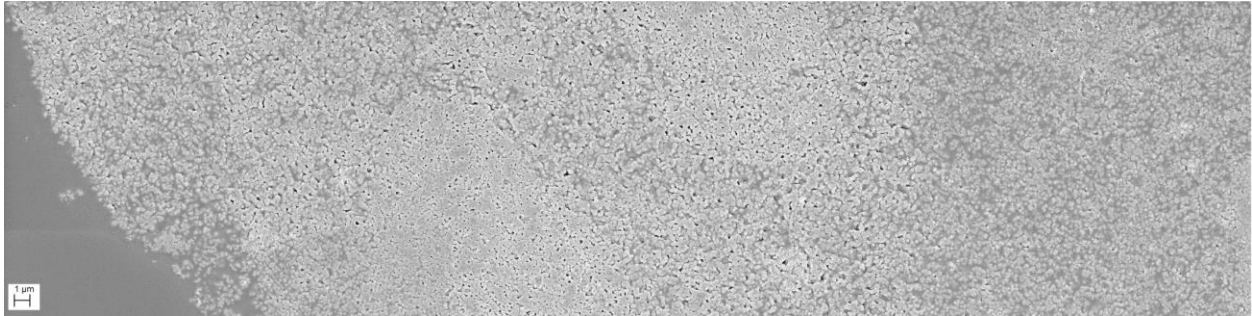


Figure 10. Mosaic of 3 images at 10,000x magnification of the outer rim of the 40 Hz and 1 mm amplitude granule sample.

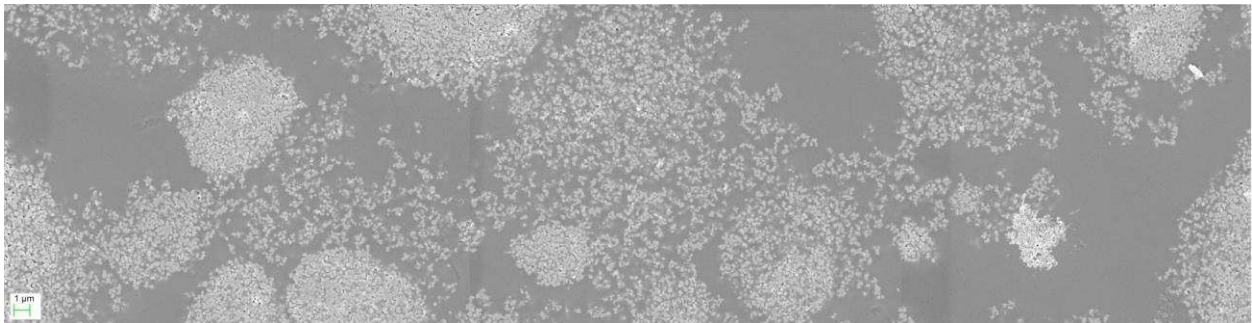


Figure 11. Mosaic of 3 images at 10,000x magnification of the inner core of the 40 Hz and 1 mm amplitude granule sample.

To obtain a quantitative measure of the change in packing fraction, the series of SEM images was used as a line scan across the granule measuring the packing fraction with spatial resolution of $27\ \mu\text{m}$ by $27\ \mu\text{m}$, or the area of the SEM image at $10,000\times$ magnification. This was

conducted using ImageJ (<http://imagej.nih.gov>) to convert each grayscale SEM image from the entire series into a binary, black-and-white image. This allowed for the actual packing fraction of each image to be calculated by dividing the number of white pixels by the total number of pixels in the image. A comparison could then be made to other images of the scan, providing a measure of the packing fraction as a function of the location across the horizontal diameter of the granule cross-section.

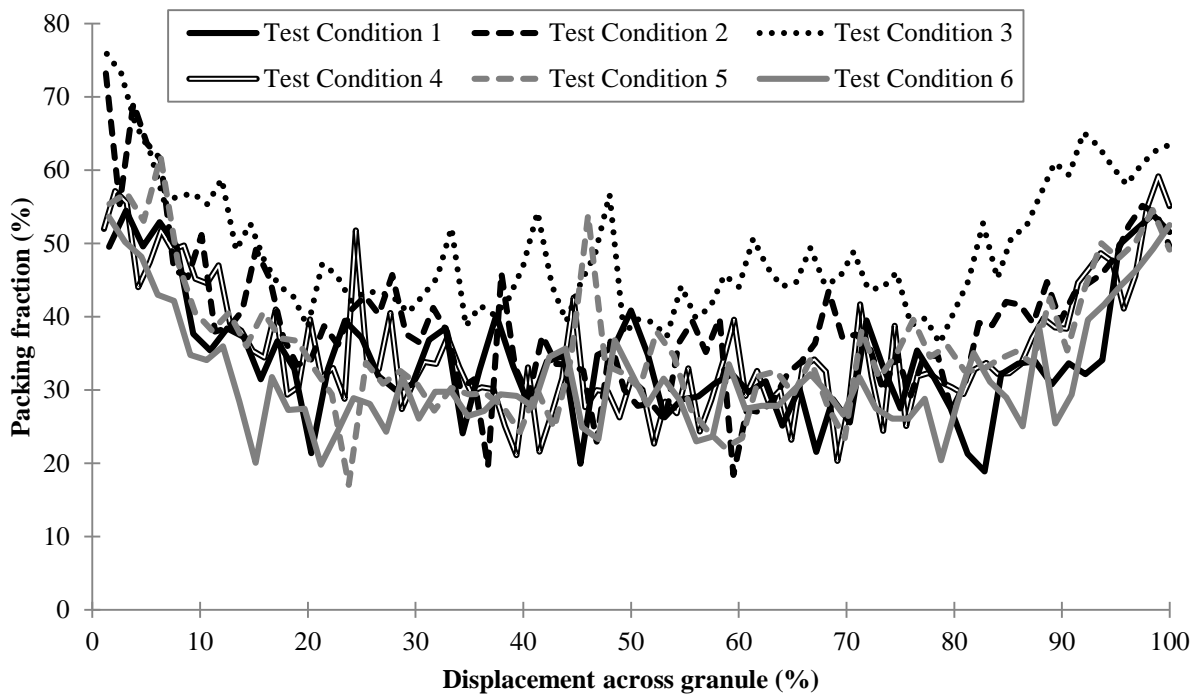


Figure 12. Packing fraction of the granule cross-section across its horizontal diameter for each vibration test condition.

The results of the scans are shown in Figure 12 for granules from all test conditions. The displacement across the granule is shown as a percentage, with 0% and 100% being the left and right edges of the granule, respectively, and 50% being the center. From the data, the packing

fraction of the granules is highest between the first and last 10% to 15% of the granule displacement. The central area of the granule produced a lower packing fraction. This leads to the conclusion that granules from all the test conditions exhibit the same core-rim microstructure, where the outer rim of the granule is at a higher density than the inner core. This conclusion is also confirmed by the SEM images in Figures Figure 10 and Figure 11. No noticeable variation of packing fraction with vibrational condition is observed.

4. Conclusions

Titania powder was shown to exhibit auto-granulation behavior under mechanical vibration. The equilibrium size of the granules produced increased linearly with increasing energy of vibration. A novel method to image the microstructure of the porous granules was developed. This method involved heat treatment and epoxy infiltration of the granules before polishing to provide a cross section exposing the hemispherical plane. The images showed a heterogeneous microstructure, with smaller clusters of particles clearly visible within the larger granules. Analysis of the particle packing fraction showed the granules exhibited a core-rim microstructure, with the center core of the granule having a lower density than the outer rim, for all vibrational intensities investigated.

References

1. Etzler, F.M. and M.N. Uddin, Powder Technology and Pharmaceutical Development: Particle Size and Particle Adhesion. Kona, 2013. **30**(125): p. 2013.
2. Mohammadi, M.S. and N. Harnby, Bulk density modelling as a means of typifying the microstructure and flow characteristics of cohesive powders. Powder Technology, 1997. **92**(1): p. 1-8.
3. Litster, J., B. Ennis, and L. Lian, The Science and Engineering of Granulation Processes. 2004: Springer.
4. Fayed, M.E. and L. Otten, Handbook of powder science and technology. 1984: Van Nostrand Reinhold Co.
5. Reed, J.S., Principles of ceramics processing. 1995: Wiley New York.
6. Ku, N., et al. Auto-granulation of fine cohesive powder by mechanical vibration. in WCPT7. 2014. Beijing.
7. Ennis, B.J., G. Tardos, and R. Pfeffer, A microlevel-based characterization of granulation phenomena. Powder Technology, 1991. **65**(1): p. 257-272.
8. Nishii, K., et al., Pressure swing granulation, a novel binderless granulation by cyclic fluidization and gas flow compaction. Powder technology, 1993. **74**(1): p. 1-6.
9. Horio, M., Binderless granulation—its potential, achievements and future issues. Powder technology, 2003. **130**(1): p. 1-7.
10. Golchert, D., et al., Effect of granule morphology on breakage behaviour during compression. Powder Technology, 2004. **143–144**(0): p. 84-96.
11. Barletta, D. and M. Poletto, Aggregation phenomena in fluidization of cohesive powders assisted by mechanical vibrations. Powder Technology, 2012. **225**: p. 93-100.
12. Zhou, L., et al., Model of estimating nano-particle agglomerate sizes in a vibro-fluidized bed. Advanced Powder Technology, 2013. **24**(1): p. 311-316.
13. Hsiau, S.S. and S.J. Pan, Motion state transitions in a vibrated granular bed. Powder Technology, 1998. **96**(3): p. 219-226.
14. Thomas, B., M.O. Mason, and A.M. Squires, Some behaviors of shallow vibrated beds across a wide range in particle size and their implications for powder classification. Powder Technology, 2000. **111**(1–2): p. 34-49.
15. Hardie, N.A., G. MacDonald, and E.W. Rubel, A new method for imaging and 3D reconstruction of mammalian cochlea by fluorescent confocal microscopy. Brain Research, 2004. **1000**(1–2): p. 200-210.
16. Barsoum, M. and W. Barsoum, Fundamentals of Ceramics. 2002: Taylor & Francis.
17. Fisher, R.A., Statistical Methods for Research Workers. 1936: Oliver & Boyd.